Propagation of ultrashort laser pulses in water: linear absorption and onset of nonlinear spectral transformation

Alexei V. Sokolov,[1] Lucas M. Naveira,[1] Milan P. Poudel,[1] James Strohaber,[1] Cynthia S. Trendafilova,[1] William C. Buck,[1] Jieyu Wang,[1] Benjamin D. Strycker,[1,*] Chao Wang,[2] Hans Schuessler,[1] Alexandre Kolomenskii,[1] and George W. Kattawar[1]

[1]Institute for Quantum Studies and Department of Physics, Texas A&M University, 4242 TAMU, College Station, Texas 77843-4242, USA

[2]Department of Biomedical Engineering, Texas A&M University, 3120 TAMU, College Station, Texas, 77843-3120, USA

*Corresponding author: bstryck2@physics.tamu.edu

Received 12 October 2009; accepted 2 December 2009; posted 6 January 2010 (Doc. ID 118399); published 20 January 2010

We study propagation of short laser pulses through water and use a spectral hole filling technique to essentially perform a sensitive balanced comparison of absorption coefficients for pulses of different duration. This study is motivated by an alleged violation of the Bouguer–Lambert–Beer law at low light intensities, where the pulse propagation is expected to be linear, and by a possible observation of femtosecond optical precursors in water. We find that at low intensities, absorption of laser light is determined solely by its spectrum and does not directly depend on the pulse duration, in agreement with our earlier work and in contradiction to some work of others. However, as the laser fluence is increased, interaction of light with water becomes nonlinear, causing energy exchange among the pulse's spectral components and resulting in peak-intensity dependent (and therefore pulse-duration dependent) transmission. For 30 fs pulses at 800 nm center wavelength, we determine the onset of nonlinear propagation effects to occur at a peak value of about 0.12 mJ/cm^2 of input laser energy fluence.

OCIS codes: 320.2250, 320.5540, 320.7110, 320.7120.

1. Introduction

Propagation of short laser pulses through water is an important research area that has recently been surrounded by a controversy concerning possible violations of the exponential attenuation law of Bouguer, Lambert, and Beer (BLB) that have been attributed to formation of femtosecond optical precursors. Optical precursors, theoretically predicted by Brillouin and Sommerfeld roughly a century ago [1], have remained largely elusive in experimental observations. As a notable exception, in recent decades precursors have been studied in media with strong and narrow absorption lines, i.e., semiconductors [2] and atomic gases [3]. Recently, optical precursors were observed while studying propagation of entangled photons through rubidium vapor [4]. However, observation of optical precursors in bulk liquids, such as water, has been a subject of substantial debate and disagreement. Choi and Österberg [5] have reported a measurement of femtosecond precursors in deionized water; in that paper, as well as in their follow-up work [6,7], Österberg and coworkers have stated that the occurrence of these precursors is associated with a violation of the exponential absorption law (BLB

0003-6935/10/030513-07$15.00/0

law). Apparently, the subsequent controversy resulted from a misunderstanding of the connection between the existence of optical precursors and the seeming violation of the BLB law even when this law was applied to each individual spectral component separately. Follow-up studies by other groups (including ours) [8–10] have experimentally shown that at low light intensities there is no noticeable deviation from the (spectral-domain) BLB law, while a spectrally varying absorption, even in the linear regime, may indeed result in nonexponential decay of the total laser pulse energy integrated over a finite spectral band.

The original claims of BLB law violations, as well as the follow-up studies that tended to disprove those claims, focused on orders-of-magnitude deviations and discrepancies and took special care to make sure the light field was sufficiently weak so as to avoid any possible sources of nonlinearity. Since this subject area is of substantial fundamental significance and has potential implications to such important applications as underwater communications and biomedical imaging, it warrants in our view further investigation. The scope of our present study is twofold: (1) We perform a balanced side-by-side comparison of water absorption for weak laser pulses of different duration, aiming to detect small (fraction of a percent level) duration-dependent differences. We employ a spectral hole filling technique developed by Warren and coworkers [11], where a short pulse and a long pulse (of the same spectral intensity at the same center wavelength but with opposite phase) are added coherently to produce a spectral distribution with a narrow gap (hole). In this situation, any pulse-duration dependent absorption is expected to result in "filling" of this hole. (2) We quantify the transition from linear to nonlinear pulse propagation in water.

We proceed by first reviewing the basics of our technique, and then we describe experimental results for pulses with peak intensities varied over many orders of magnitude. Electric fields of two coherent laser pulses (a short and a long one) of the same spectral intensity at the same center frequency ω_c, but with opposite phase, add up to produce a spectrum with a hole [Fig. 1(a)], since at ω_c the two contributions exactly cancel:

$$E(\omega) = A\left(\exp\left[-\frac{(\omega-\omega_c)^2}{8\ln(2)}\tau_1^2\right] - \exp\left[-\frac{(\omega-\omega_c)^2}{8\ln(2)}\tau_2^2\right]\right), \tag{1a}$$

$$E(t) = B\left(\exp\left[-2\ln(2)\left(\frac{t}{\tau_1}\right)^2\right] - \frac{\tau_1}{\tau_2}\exp\left[-2\ln(2)\left(\frac{t}{\tau_2}\right)^2\right]\right)\cos(\omega_c t), \tag{1b}$$

where $E(\omega)$ is the spectral amplitude, $E(t)$ is the amplitude of the electric field [$I = |E(t)|^2$ is shown schematically in Fig. 1(b)], and τ_1 and τ_2 are the intensity full width at half-maximum (FWHM) pulse durations. When the resultant waveform is sent through a linear absorbing or scattering medium, this balance will persist if the absorption is independent of pulse duration. Any absorption that would affect the longer and shorter pulses differently would inevitably destroy the perfect destructive interference at the center wavelength and result in the filling of the spectral hole.

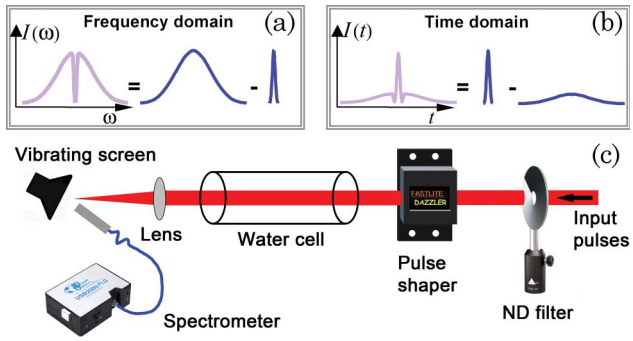

Fig. 1. (Color online) Spectral-hole-filling experiment: (a) Frequency domain and (b) time domain schematics. (c) Experimental setup (femtosecond laser oscillator not shown). Initial 7 fs laser pulses pass through the pulse shaper, which produces a spectral hole and reduces the total spectral bandwidth, and enter the water cell. The transmitted spectra are measured by the spectrometer.

Figure 1(c) shows a typical setup for a spectral-hole-filling experiment, where a pulse shaper is used to obtain the required waveforms, and the spectra transmitted through the sample are measured by a spectrometer.

Before proceeding further, we need to make a note on the rapid dispersion of short laser pulses in water; a detailed discussion of this phenomenon is included in Appendix A. Although a plethora of virtues of ultrashort laser pulses have been discovered, their duration depends on the medium dispersion, their spectral bandwidth, and the propagation distance. Because of the large spectral width of these pulses, we had to investigate the effect of the glass window of our water cell on the shape and duration of a pulse as it emerges from the cell window and enters the water. Our simulations (see Appendix A) show that an initial 7 fs pulse broadens significantly faster than a 30 fs pulse and becomes longer than the latter even for a 2 mm thick glass window. Therefore, in order to obtain a 7 fs pulse at the entrance of our water cell, the pulse has to be prechirped to compensate for the dispersion in the glass window. Note that a similar effect of fast pulse spreading due to dispersion also takes place in the water itself. Therefore, even though our femtosecond oscillator was capable of producing pulses as short as 7 fs, in our experiments we chose to limit the total pulse bandwidth and work with pulses of not less than 25 fs duration.

2. Experiments with Femtosecond Oscillator Pulses

To study spectral hole filling experimentally, we use an ultrabroadband mode-locked femtosecond

Ti:sapphire oscillator (Rainbow, FemtoLasers) followed by an acousto-optic programmable pulse shaper (Dazzler, FastLite) to obtain a broad, smooth spectrum with a spectral hole whose position and width can be precisely controlled. The laser oscillator produces pulses of 7 fs duration with a spectrum that extends from 660 to 980 nm; its average output power is 340 mW, and the repetition rate is 78 MHz, so that the energy per pulse is about 4 nJ. We set the Dazzler to reduce the full spectral bandwidth to 80 nm. The width of the hole is chosen to be 10 nm, and for three measurements its center is positioned at three different wavelengths, i.e., at 767 nm, 800 nm, and 827 nm [example spectra can be seen in Figs. 2(a)–2(c)]. Note that the pulse shaper is capable of compensating additional dispersion (including its own dispersion) and therefore allows synthesis of transform-limited waveforms. Assuming a constant spectral phase, we calculate pulse shapes (not shown), which indeed contain long- and short-duration components (200 fs and 25 fs, respectively), as drawn in Fig. 1(b).

The resultant shaped pulses are directed to a cylindrical glass cell (1.5 m length) containing distilled water. Laser light emerging from the water cell is focused by a lens and scatters off a white screen vibrating at a 50 Hz rate; then a fraction of it couples into a fiber and is detected by a spectrometer (USB 2000, Ocean Optics), as shown in Fig. 1(c). This configuration is used in order to make the measurement insensitive to small variations of laser beam alignment; the screen vibration reduces the possible effects of intensity speckles and diffraction that result in fluctuating modulations of the measured spectrum. We check that the reshaping of the spectra [water cell input, Figs. 2(a)–2(c), versus output, Figs. 2(d)–2(f)] is mostly consistent with linear absorption in water (which is strongly wavelength dependent), although these present experiments are not optimized for measuring the wavelength-dependent absorption as reliably as some of our earlier experiments were [10].

We vary laser power at the input of the water cell from 1 mW to 12 mW in 1 mW increments using a neutral density filter while recording the output spectra [Figs. 2(d)–2(f)]. To compare the shapes of the spectra for different input powers, we first take the data and divide each measured spectral curve by the

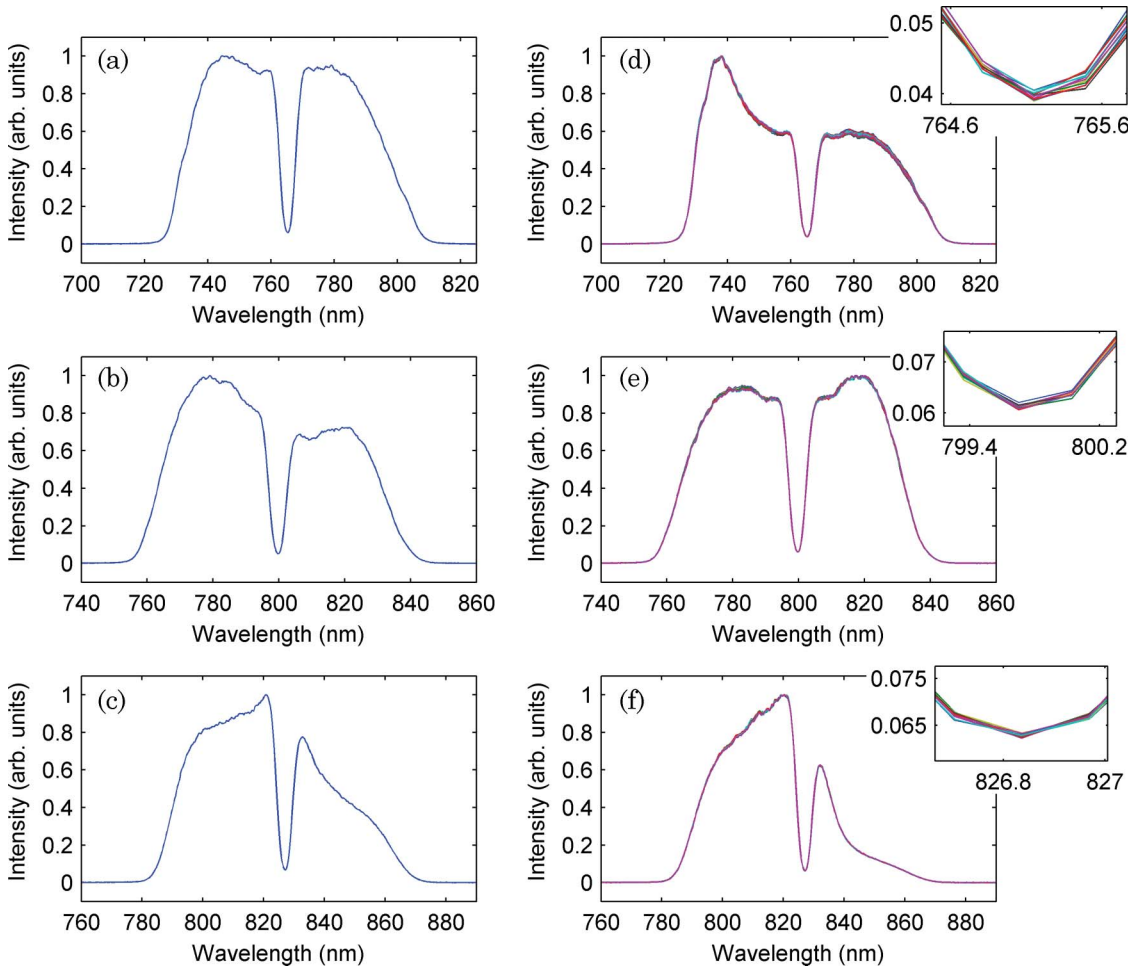

Fig. 2. (Color online) Results from the spectral hole filling experiment with low-power (laser oscillator) shaped pulses. Parts (a)–(c) show input spectra with the spectral hole centered at (a) 767 nm, (b) 800 nm, and (c) 827 nm wavelengths. Parts (d)–(f) show the corresponding output spectra after propagation through 1.15 m of distilled water; insets show zoomed-in spectral hole regions.

corresponding input power. This procedure by itself produces curves deviating from each other by no more than the relative uncertainty of our power measurements (with the absolute experimental uncertainty of 0.1 mW, the relative uncertainty varies from 10% for 1 mW of input power to 0.8% for 12 mW). To avoid these variations due to uncertainty in the power measurements, we normalize each curve to its peak value, in order to be able to look at possible small (well less than 1%) relative variations in the resultant spectral shapes. The insets shown in Figs. 2(d)–2(f) illustrate an essential absence of a mismatch among different curves at the spectral hole wavelengths. This mismatch is less than 0.1% of the peak value and is within the spectrometer noise.

The above results, to within our precision of 0.1% showing no "hole filling," indicate that absorption affects a 25 fs pulse exactly the same way it affects a 200 fs pulse. For a linear regime this is as expected, since new frequency components can only appear as a result of nonlinear generation. Simple estimates show that in the experiments with the oscillator pulses, we are well below intensity levels required for any nonlinear effects (i.e., self-focusing or self-phase modulation) to occur.

3. Experiments with Amplified Pulses: Transition to the Nonlinear Regime

To investigate the propagation of laser pulses in a broad range of intensities and to quantify the transition to nonlinear behavior, we used amplified laser pulses. Figure 3 shows a schematic of our experimental setup: after amplification (Femtopower multipass system from Femtolasers) a spectral hole with the central wavelength of 794 nm is produced in the pulse spectrum by placing an obstruction that blocks a narrow spectral interval in the compressor (see Fig. 3). The resultant spectrum is centered at 800 nm, and has a total bandwidth of about 70 nm and a spectral hole width of 20 nm (corresponding to 30 fs and 100 fs pulse durations, respectively). The pulse repetition rate is 5 kHz. The laser pulses propagate through a variable neutral density filter and then through a telescope, which reduces the beam size by a factor of 3 (to a waist of 2.1 mm). The collimated laser beam passes through the glass window and enters the water sample. After propagating the single-pass length of 1.15 m in distilled water, the pulses are scattered off of a vibrating white screen and measured with a fiber-coupled spectrometer, similar to the above-described experiment with laser oscillator pulses. The input power is measured by redirecting the laser beam to a powermeter (Nova II, Ophir) with a removable mirror just before the water cell.

Figure 4(a) shows the dependence of the transmitted pulse spectrum on the input power. Each curve has been normalized to the peak value of the spectrum obtained at 340 mW of input power. The curves are vertically displaced, with greater input powers corresponding to greater upward vertical displacement. It can be seen that, as input power increases, the hole begins to fill in and also shifts somewhat from the initial wavelength of 794 nm toward smaller wavelengths at higher input powers.

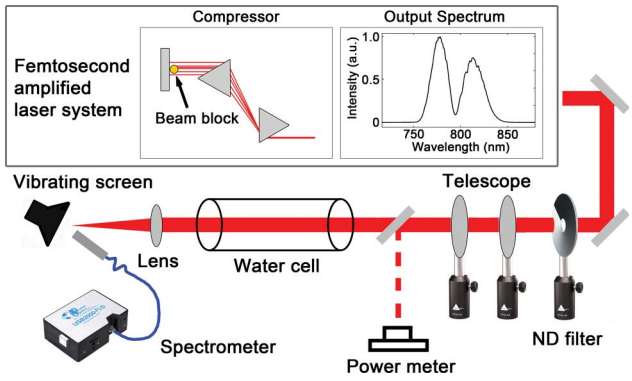

Fig. 3. (Color online) Experimental setup for measuring propagation of amplified laser pulses through water. An obstruction is placed in the compressor to produce a hole in the laser spectrum. Then the pulses propagate through the water cell, and the transmitted spectra are measured by the spectrometer.

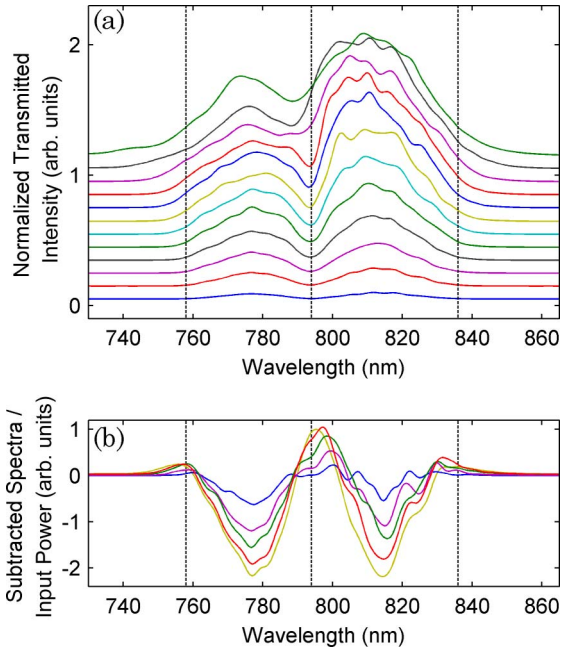

Fig. 4. (Color online) Transformation of transmitted spectra with increasing input laser power: (a) Measured spectra. To aid in visualization, each spectrum has been vertically displaced, with larger upward vertical displacements corresponding to larger input powers. The input powers for the shown spectra are, from bottom to top: 5 mW, 15 mW, 25 mW, 40 mW, 60 mW, 80 mW, 100 mW, 120 mW, 140 mW, 180 mW, 250 mW, and 340 mW. (b) Changes in the spectrum, relative to spectra expected for linear transmission and calculated by scaling the output spectrum obtained for 20 mW input power. These curves are obtained by subtracting the expected linear-transmission spectra from the actual measured spectra, dividing by the input power, and scaling relative to the peak value obtained in the 200 mW curve. The input powers shown, with increasing spectral transformation, are 40 mW, 80 mW, 120 mW, 160 mW, and 200 mW. In both (a) and (b), dotted vertical lines correspond to wavelengths of 794 nm (spectral hole center at low power), and two wavelengths at the wings of the spectrum, 758 and 836 nm.

In addition, the wings of the spectrum experience broadening. Figure 4(b) shows the differential changes of the spectrum at different power levels. Each of the shown curves was obtained with the following procedure: a spectrum, calculated assuming linear behavior, is subtracted from the measured spectrum and divided by the input power; each resultant curve is then scaled relative to the obtained peak value of the curve corresponding to an input power of 200 mW. As can be seen in the figure, the energy from the intense spectral components is transferred to the hole and wings (i.e., to spectral components of low intensity) as the input power increases. We note that this behavior is reminiscent of diffusion, with a spectral diffusion coefficient increasing with the laser power.

Figure 5 shows the measured transmitted spectral intensities at three wavelengths (marked in Fig. 4 by dotted vertical lines) as a function of the input power. The three wavelengths correspond to the low-power spectral hole center (794 nm) and two wavelengths at the spectral wings (758 and 836 nm) having, at low input powers, the same spectral intensity as the hole center. At low input powers (below about 40 mW), we observe linear growth of the spectral intensities, turning to nonlinear behavior at higher input powers.

This behavior can be seen especially clearly on the logarithmic plot of the transmitted spectral intensity at the hole central wavelength of 794 nm as a function of the input power (see Fig. 6). A significant (1% compared to the peak spectral intensity) deviation from the linear behavior starts at around 40 mW power, which correspond to a peak value of 0.12 mJ/cm^2 of input laser energy fluence and, given the pulse durations used, to a peak intensity of about 10^{10} W/cm^2. Above input powers of 40 mW, the spectral intensity at 794 nm exhibits quadratic growth. A new drastic change in the behavior happens at around 250 mW (which corresponds, for the parameters of our experiment, to a peak input fluence of 0.73 mJ/cm^2).

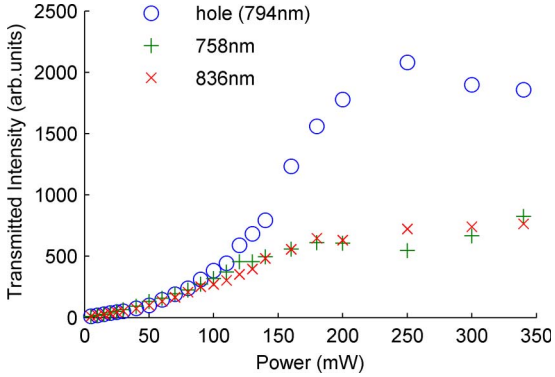

Fig. 5. (Color online) Transmitted intensity for three wavelengths as a function of input laser power. The three wavelengths correspond to the low-power spectral hole center (794 nm) and two wavelengths at the spectral wings (758 and 836 nm) having, at low input powers, the same spectral intensity as the hole center.

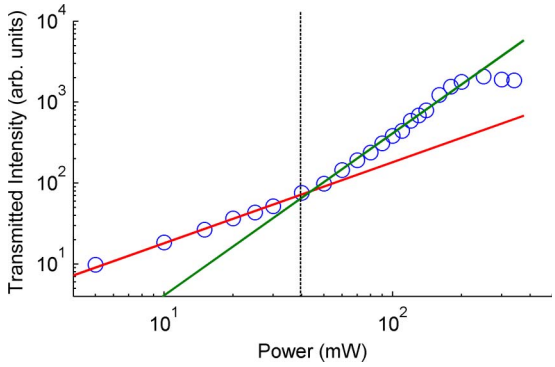

Fig. 6. (Color online) Plot on a log-log scale of transmitted spectral intensity at 794 nm (initial spectral hole center) as a function of the input power. The blue circles show the measured data. The red reference line has a slope of 1 and fits well to the data points in the low-power region, indicating a linear dependence. The green reference line has a slope of 2 and fits the data points in the region of intermediate power up to about 250 mW, indicating a quadratic dependence. The change from the linear dependence to quadratic dependence can be clearly seen at around 40 mW (where a dotted vertical line is drawn).

The quadratic power dependence may result from a third-order nonlinear mixing process (please note that second-order nonlinearities are forbidden in centrosymmetric media such as liquid water). As a likely possibility, we consider two-photon processes such as stimulated Raman scattering (SRS). At powers above 100 mW we find that the spectral hole position (the location of the minimum in the output spectrum) shifts toward shorter wavelengths; this behavior is also consistent with SRS, which converts shorter-wavelength photons to longer-wavelength ones. It should be pointed out that even though SRS is a likely process to come into play first, as the laser intensity is gradually increased, many other phenomena such as thermal lensing, self-focusing, self-phase modulation, and medium ionization all become significant at somewhat higher intensities [12–14]. In our experiment we observe an interplay of these effects at powers above 250 mW; however, detailed investigation of these phenomena is beyond the scope of our present work.

4. Conclusion

We have investigated propagation of femtosecond laser pulses with the central wavelength around 800 nm in water by employing a spectral hole filling technique. We showed experimentally and with precision of better than 0.1% that there is no pulse-duration dependent absorption for ultrashort pulses of duration around 30 fs in the linear light–matter interaction regime. We then quantified the transition of such pulse behavior from the linear to the nonlinear interaction regime, and we found that this transition occurs at around 0.12 mJ/cm^2. Above this value a quadratic growth of the intensity at the spectral hole was observed up to about 0.73 mJ/cm^2. Also, we found that as the light–matter interaction becomes increasingly nonlinear, the location of the minimum in the

output spectrum shifts toward shorter wavelengths. We suggest stimulated Raman scattering as a possible mechanism for this spectral hole filling and shifting effect. However, it should be pointed out that many other phenomena, such as thermal lensing, self-focusing, self-phase modulation, and medium ionization, can affect propagation of short and intense laser pulses in the nonlinear regime, and the detailed investigation of these mechanisms is certainly out of the scope of this paper.

The main conclusion is that no violations of the BLB law in the linear light–matter interaction regime was registered in this work. It may still be a matter of debate whether pulses of any duration, most significantly durations that are a small fraction of the vibrational periods of water molecules, will induce a violation of the BLB law; however, we can now state that none have yet been documented. As we have shown, due to dispersion, ultrashort pulses become increasingly fragile as their duration decreases, so that they can maintain their pulse duration on correspondingly decreasing distances (less than a millimeter for sub-10 fs pulses), unless a special compensation of the dispersion spreading is implemented.

Appendix A

Ultrashort femtosecond pulse broadening is investigated here. We consider sufficiently low incident laser intensities to involve only linear response of the media under study. The electric field of a pulse results from a superposition of its Fourier components:

$$E(z,t) = \frac{1}{2\pi}\int_{-\infty}^{\infty} E(\omega)\ \exp[i(k(\omega)z - \omega t)]\mathrm{d}\omega, \qquad \text{(A1)}$$

where we assume that the pulse is propagating in the positive z direction and regard its divergence due to diffraction as negligible, $E(z,t)$ is the electric field, ω is the angular frequency, z is the propagation distance in the medium, t is time, $E(\omega)$ is the Fourier component (or complex spectral amplitude) of the incident pulse at the input interface of the considered dielectric medium (at $z = 0$), and $k(\omega)$ is the complex wave vector in an absorptive medium such as water. Usually, the obtainable data characteristic of the medium are the refractive index $n(\omega)$ and the absorption coefficient $\alpha(\omega)$ instead of the wave vector $k(\omega)$. The relations between $k(\omega)$, the refractive index $n(\omega)$, and the absorption coefficient $\alpha(\omega)$ are $\mathrm{Re}[k(\omega)] = [n(\omega)\omega]/c$ and $\mathrm{Im}[k(\omega)] = \alpha(\omega)/2$.

We consider the broadening of pulse duration of an ultrashort pulse passing through a glass window and a water cell. In our simulation, we use documented refractive indices of BK7 glass and water. The refractive index $n(\lambda)$ of BK 7 glass follows the Sellmeier equation [15]:

$$n(\lambda) = \sqrt{1 + \frac{B_1\lambda^2}{\lambda^2 - C_1} + \frac{B_2\lambda^2}{\lambda^2 - C_2} + \frac{B_3\lambda^2}{\lambda^2 - C_3}}, \qquad \text{(A2)}$$

where λ is the wavelength of light, $B_1 = 1.03961212\,\mu\mathrm{m}^{-2}$, $B_2 = 2.31792344 \times 0.1\,\mu\mathrm{m}^{-2}$, $B_3 = 1.01046945\,\mu\mathrm{m}^{-2}$, $C_1 = 6.00069867 \times 0.001\,\mu\mathrm{m}^2$, $C_2 = 2.00179144 \times 0.01\,\mu\mathrm{m}^2$, and $C_3 = 1.03560653 \times 100\,\mu\mathrm{m}^2$.

The refractive index of water is given by Quan and Fry [16]:

$$n(\lambda) = 1.31279 + 15.762\lambda^{-1} - 4328\lambda^{-2} + 1.1455 \times 10^6\lambda^{-3}, \qquad \text{(A3)}$$

where λ is in nanometers. This formula is verified by the experimental data of [17] in a range of 200 to 1100 nm. The absorption coefficient is obtained from the data of Kou, *et al.* [18] and Pope and Fry [19], which in combination cover the range from 380 to 2500 nm.

The pulse duration is defined as the full width at half-maximum (FWHM) of the pulse intensity:

$$I(z,t) = E(z,t)E(z,t)^*. \qquad \text{(A4)}$$

In our simulation, we assume a pulse with a duration τ_0 and a carrier frequency ω_c in the form

$$E(0,t) = \frac{1}{\sqrt{2\pi}}\ \exp\left[-\frac{2\ \ln(2)\ t^2}{\tau_0^2}\right]\cos(\omega_c t). \qquad \text{(A5)}$$

The spectral amplitude $E(\omega)$ is obtained by the Fourier transformation of Eq. (A5):

$$E(\omega) = \exp\left[-\frac{(\omega-\omega_c)^2\tau_0^2}{8\ \ln(2)}\right] = \exp\left[-\gamma(\omega-\omega_c)^2\right]. \qquad \text{(A6)}$$

We define $\gamma = \tau_0^2/[8\ \ln(2)]$. After propagating a certain distance z, the phase delays between different spectral components determine the pulse broadening. Using the carrier frequency ω_c as a reference, the phase difference of $ik(\omega)z - i\omega t$ can be expressed as a Taylor expansion:

$$(izb_1 - it)(\omega-\omega_c) + \left(\frac{izb_2}{2}\right)(\omega-\omega_c)^2 + \ldots, \qquad \text{(A7)}$$

where $b_j = \mathrm{d}^j k(\omega)/\mathrm{d}\omega^j|_{\omega_c}$ and $j = 1, 2, 3\ldots$. The group velocity dispersion (GVD) approximation keeps the expansion to the second order and is given by $\mathrm{GVD} = \mathrm{d}^2k(\omega)/\mathrm{d}\omega^2|_{\omega_c}$. Therefore, the value of GVD equals b_2. By substituting the GVD approximation into Eq. (A1), an analytic solution of the intensity envelope is obtained:

$$I(z,t) \sim \exp\left[-\frac{2\gamma(t-zb_1)^2}{4\gamma^2 + z^2b_2^2}\right]. \qquad \text{(A8)}$$

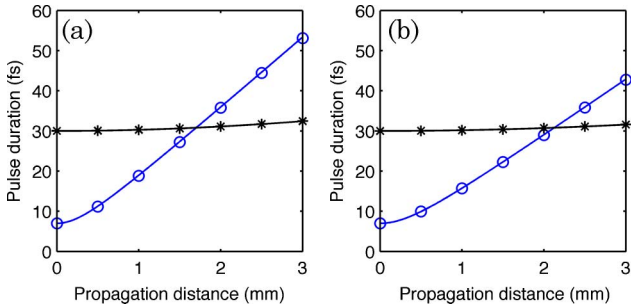

Fig. 7. (Color online) Calculated pulse duration versus propagation distance (a) in K7 glass and (b) in water for two transform-limited input pulses of 7 fs (blue lines and circles) and 30 fs (black lines and stars) initial duration (both at an 800 nm center wavelength). In both figures, the data points show the results calculated with the actual wavelength-dependent refractive indices, while the lines are obtained with the group velocity dispersion (GVD) approximation.

Since $b_2 = \mathrm{GVD}$ and $\gamma = \tau_0^2/8\ \ln(2)$, we are led to a hyperbolic relation between the pulse duration τ and the propagation distance z:

$$\tau(z) = \sqrt{\tau_0^2 + \left(\frac{4\ \ln(2)\mathrm{GVD}}{\tau_0}\right)^2 z^2}. \qquad \text{(A9)}$$

Shown in Fig. 7 are the simulation results obtained for pulses with initial durations of 7 and 30 fs, both centered at 800 nm.

This work was supported by the Office of Naval Research (ONR) under contract N00014-08-1-0037 and the Defense University Research Initiative Program (DURIP) under contract N00014-08-1-0804, and in part by National Science Foundation (NSF) grants 0722800 and 354897, Texas Advanced Research Program grant 010366-0001-2007, Army Research Office grant W911NF-07-1-0475, and Robert A. Welch Foundation grant A1547. We also wish to thank Matthew Springer for his help with the manuscript.

References

1. L. Brillouin, *Wave Propagation and Group Velocity* (Academic, 1960).
2. J. Aaviksoo, J. Kuhl, and K. Ploog, "Observation of optical precursors at pulse propagation in GaAs," Phys. Rev. A **44**, R5353–R5356 (1991).
3. H. Jeong, A. M. C. Dawes, and D. J. Gauthier, "Direct observation of optical precursors in a region of anomalous dispersion," Phys. Rev. Lett. **96**, 143901 (2006).
4. S. Du, C. Belthangady, P. Kolchin, G. Y. Yin, and S. E. Harris, "Observation of optical precursors at the biphoton level," Opt. Lett. **33**, 2149–2151 (2008).
5. S. H. Choi and U. Österberg, "Observation of optical precursors in water," Phys. Rev. Lett. **92**, 193903 (2004).
6. U. J. Gibson and U. L. Osterberg, "Optical precursors and Beer's law violations: nonexponential propagation losses in water," Opt. Express **13**, 2105–2110 (2005).
7. A. E. Fox and U. Osterberg, "Observation of nonexponential absorption of ultra-fast pulses in water," Opt. Express **14**, 3688–3693 (2006).
8. J. C. Li, D. R. Alexander, H. F. Zhang, U. P. Parali, D. W. Doerr, J. C. Bruce III, and H. Wang, "Propagation of ultrashort laser pulses through water," Opt. Express **15**, 1939–1945 (2007).
9. Y. Okawachi, A. D. Slepkov, I. H. Agha, D. F. Geraghty, and A. L. Gaeta, "Absorption of ultrashort optical pulses in water," J. Opt. Soc. Am. A **24**, 3343–3347 (2007).
10. L. M. Naveira, B. D. Strycker, J. Wang, G. O. Ariunbold, A. V. Sokolov, and G. W. Kattawar, "Propagation of femtosecond laser pulses through water in the linear absorption regime," Appl. Opt. **48**, 1828–1836 (2009).
11. M. C. Fischer, H. C. Liu, I. R. Piletic, and W. S. Warren, "Simultaneous self-phase modulation and two-photon absorption measurement by a spectral homodyne *Z*-scan method" Opt. Express **16**, 4192–4205 (2008).
12. N. Tcherniega, A. Sokolovskaia, A. D. Kudriavtseva, R. Barille, and G. Rivoire, "Backward stimulated Raman scattering in water," Opt. Commun. **181**, 197–205 (2000).
13. A. Brodeur and S. L. Chin, "Band-gap dependence of the ultrafast white-light continuum," Phys. Rev. Lett. **80**, 4406–4409 (1998).
14. M. Koselik, G. Katona, J. V. Moloney, and E. M. Wright, "Theory and simulation of supercontinuum generation in transparent bulk media," Appl. Phys. B **77**, 185–195 (2003).
15. "Optical glass data sheets," Schott, Inc., http://www.us.schott.com/advanced_optics/english/download/datasheet_all_us.pdf
16. X. Quan and E. S. Fry, "Empirical equation for the index of refraction of seawater," Appl. Opt. **34**, 3477–3480 (1995).
17. P. D. T. Huibers, "Models for the wavelength dependence of the index of refraction of water," Appl. Opt. **36**, 3785–3787 (1997).
18. L. Kou, D. Labrie, and P. Chylek, "Refractive indices of water and ice in the 0.65 to 2.5 μm spectral range," Appl. Opt. **32**, 3531–3540 (1993).
19. R. M. Pope and E. S. Fry, "Absorption spectrum (380–700 nm) of pure water. II. Integrating cavity measurements," Appl. Opt. **36**, 8710–8723 (1997).